UNCLASSIFIED

ANL-5079
Metallurgy & Ceramics

ARGONNE NATIONAL LABORATORY
P. O. Box 299
Lemont, Illinois

DEPOSITION OF CORROSION PRODUCTS BY CATAPHORESIS

by

Walter Fagan

REACTOR ENGINEERING DIVISION

June 25, 1953

Operated by The University of Chicago
under
Contract W-31-109-eng-38

UNCLASSIFIED

DISCLAIMER

This report was prepared as an account of work sponsored by an agency of the United States Government. Neither the United States Government nor any agency Thereof, nor any of their employees, makes any warranty, express or implied, or assumes any legal liability or responsibility for the accuracy, completeness, or usefulness of any information, apparatus, product, or process disclosed, or represents that its use would not infringe privately owned rights. Reference herein to any specific commercial product, process, or service by trade name, trademark, manufacturer, or otherwise does not necessarily constitute or imply its endorsement, recommendation, or favoring by the United States Government or any agency thereof. The views and opinions of authors expressed herein do not necessarily state or reflect those of the United States Government or any agency thereof.

DISCLAIMER

Portions of this document may be illegible in electronic image products. Images are produced from the best available original document.

TABLE OF CONTENTS

DEPOSITION OF CORROSION PRODUCTS BY CATAPHORESIS

by

Walter Fagan

ABSTRACT

This report is a record of experimentation conducted intermittently over a period of two years and directed toward preventing deposition of transport corrosion products on fuel elements and other critical components in high-temperature, circulating water nuclear reactor. It includes the postulated mechanism for deposition, a description of experimental equipment, experimental data, results obtained from the experiments, and recommendations for future study.

I.   INTRODUCTION

In the Spring of 1951, an investigation was initiated to develop methods of preventing deposition of transport corrosion products on fuel elements and other critical components of a circulating water nuclear reactor. Experimental evidence[1] indicated that deposition could occur on fuel elements with disastrous results to both heat transfer and pressure drop in a reactor core. The deposition observed was similar to those where iron filings are used to observe the magnetic field of a horseshoe magnet. The observations suggested that the phenomenon of deposition was electric or magnetic in nature.

It is well known that a fluid flowing at a high velocity past a surface may cause an electric charge separation at the surface. This is known as a streaming potential. Another phenomenon that is well known is cataphoresis, the migration of colloidal particles in an electric field, the charge of the colloid being due to the absorption of ions. It seems possible that colloidal transport corrosion products could acquire an electric charge and be deposited on a metallic surface at high velocity.

II.   PURPOSE

The purpose of the investigation was to design an apparatus which would confirm the postulated deposition mechanism by inducing or preventing precipitation in preselected areas in the apparatus.

III.   TEST APPARATUS AND PROCEDURE

The test assembly, shown in Figure 1, consisted of four test sections, in series (Figure 2), housed in a 2-foot length of Schedule 80, 4-inch Type 347 stainless steel pipe with 2500-lb flanges on each end. The first test section,

---

[1]C. Wohlberg, F. W. Kleimola, "Factors Which Affect Formation and Deposition of Transport Corrosion products in High-Temperature Recirculating Water Loops," RED Technical Memorandum 2, ANL-HE-1478, June 5, 1952.
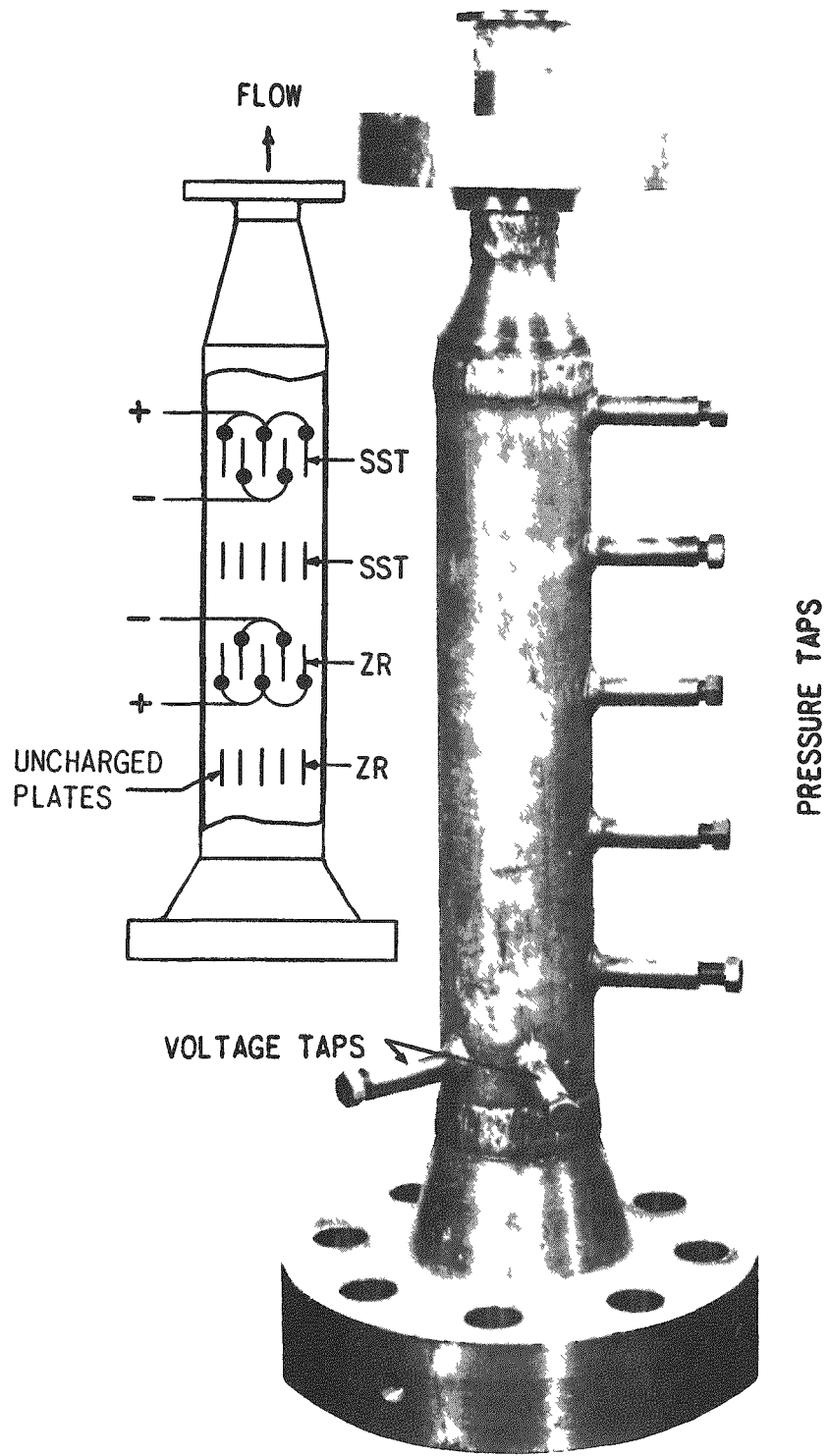
FIG. I
HIGH-PRESSURE TEST ASSEMBLY
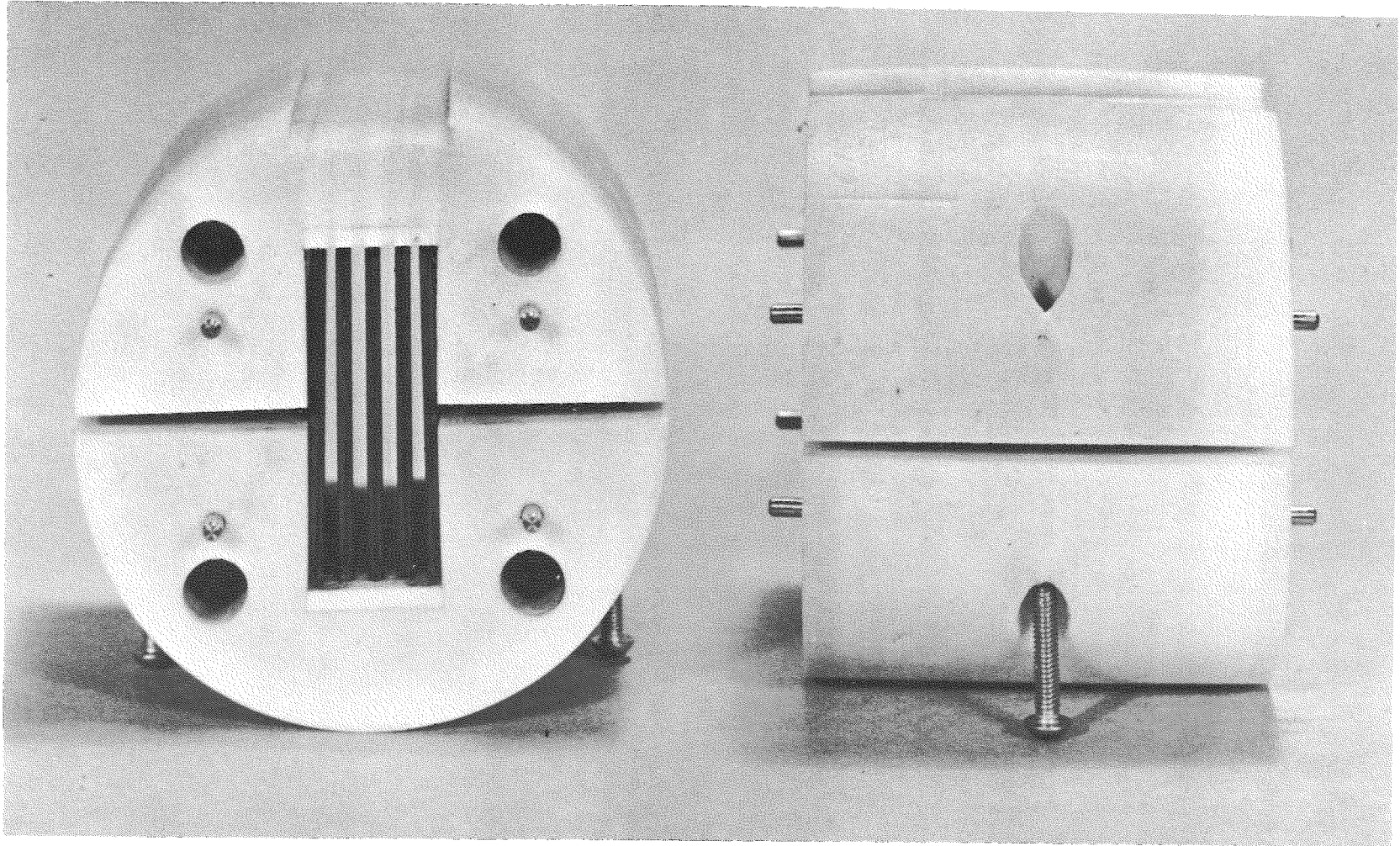
FIG. 2
PARTIAL DISASSEMBLY OF TEST SECTION

which circulating water first enters, consists of a stack of five crystal bar zirconium flat plates followed by a second identical test section except that a potential difference is externally applied across the plates (Figure 3). Test sections 3 and 4 are identical to 1 and 2 except Type 347 stainless steel plates are used. The uncharged plates in Sections 1 and 3 are electrically floating. All plates are mounted in a Teflon holder. Each of the four test plate sections is separated from its neighbors by a Teflon spacer of length 1.25 in. (Figure 4). The plates measure 2.50 in. long by 2.25 in. wide by 0.100 in. thick and are so inserted in the holder that the fluid moving parallel to the plates must travel past a 2.50 in. long plate. The holder and plates are so spaced that the cross-sectional area available for flow will be 4 rectangles, each measuring 0.087 in. by 2.0 in. Pressure drop measurements across the individual plate sections are made by means of hypodermic needles acting as pressure taps and extending into the Teflon spacer (Figure 5). Pressure drop readings are taken with a high-pressure, mercury-glass U-tube. A valve manifold is used to feed the four different pressure drops into the one U-tube. The d-c source for potential input is 1-1/2 volt dry cells and potential rheostat. A milliameter measures the current drawn by the plate sections. The test assembly may be inserted in any high-pressure, circulating water loop by merely providing two companion flanges to accommodate the test assembly. Thus the water flowing in the loop must pass through the pipe section which, in turn, houses the test assembly.

The experiment is performed by bolting the pipe section into place and circulating water through the test section. The flow rate is adjusted so that the desired fluid velocity is obtained. The cross section available for flow is such that a linear velocity of 25 fps, which corresponds to a flow rate of 54 gpm, is attained. The potential input is turned on and maintained constant at the desired value. Milliameter readings are taken periodically. It was desired in all tests that the impressed voltage would not exceed the decomposition voltage of water, although this might be a good way of preventing deposition by bubble formation assuming that the anode does not dissolve. The temperature of the loop is raised to the optimum value and maintained throughout the test. It is deemed unwise to exceed 450F owing to the dimensional instability of Teflon at high temperature under the dynamic load.

Pressure drop data are taken periodically and used as a measure of deposition. The drop is mainly due to the increase in surface roughness as caused by the deposition.

A.   Test No. 1 (Preliminary Test)

The cataphoresis pipe section was inserted in a Small Scale Heat Throughput Loop used to circulate high-pressure, high-temperature water through Type 347 stainless steel piping. Operations were not very steady with many shutdowns, down time and other perturbations. However, the total test time was 32 hr at a temperature of 240F and a pressure of 315 psig. The flow rate was 50 fps. A d-c voltage of 1.5 was impressed on the charged plates. In order to determine if decomposition of water was taking place due to elec-

NEGATIVE PLATES

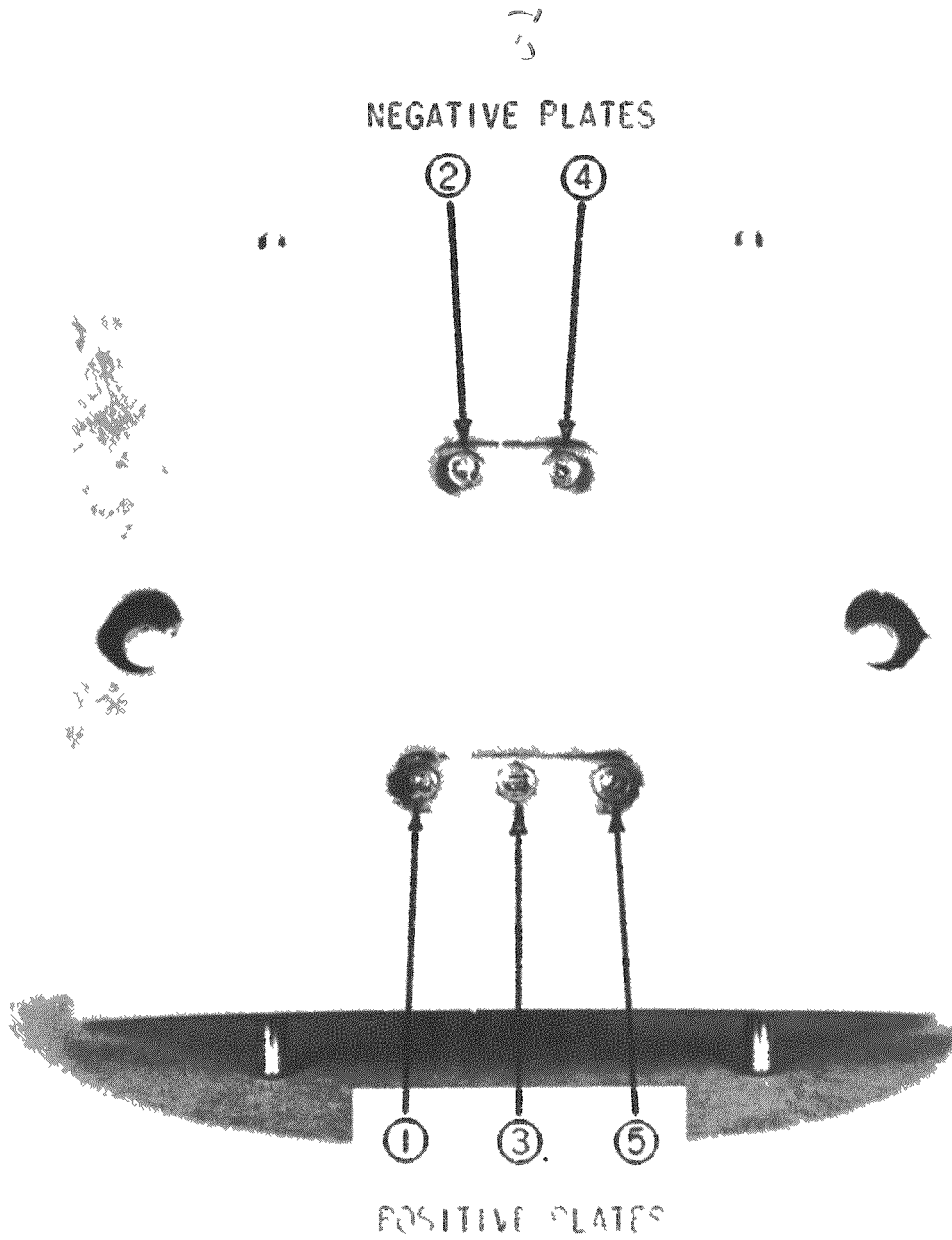POSITIVE PLATES

FIG. 3
VOLTAGE TERMINALS THROUGH TEFLON

PRESSURE TAP OPENING ⟶

FIG. 4
TEFLON SPACER
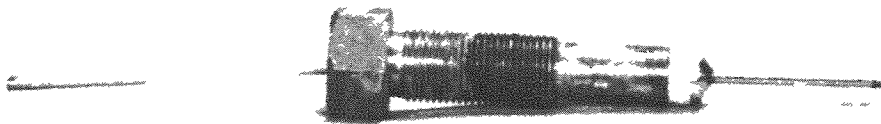
VOLTAGE TAP

PRESSURE TAP

FIG. 5
TAPS USED FOR VOLTAGE AND PRESSURE DROP MEASUREMENTS

trolysis, the current-voltage relation was plotted while the apparatus was in operation. Up to and including a voltage of 1.5, the curve is linear, having a negative intercept on the zero voltage ordinate due to a back emf. The linearity proves that electrolysis was not taking place

Since the operating conditions were so variable and so far away from optimum, and since the operating time was so short, detailed results will not be reported since they are rather meaningless and only show trends.

All uncharged plates all of the charged zirconium plates and the negatively charged stainless steel plates were clean and bright, while the positively charged stainless steel plates had a tightly adherent dark brown film on them (Figure 6). Spectrographic analysis was made of this film; the relative weights of the constituents are tabulated.

Fe	8	Mg	0.05
Pb	20	Ca	0.05
Cr	0.8	Zr	<0.05
Ni	0.7	Cu	1.0
Mn	1.0		

B.   Test No.2 (Bilgewater Test)

The preliminary test showed that a preferential precipitation was obtained, therefore it was decided to conduct the same experiment under much more favorable operating conditions. The previously described test section was inserted in a Large Scale Component Test Facility which is used to circulate high-temperature, high-pressure water through Type 347 stainless steel piping. The test was operated continuously for 362 hr. The operating conditions were:

Voltage	1.0
Velocity, fps	27
Temperature, F	450
Pressure, psi	1000
pH	6 to 7
Oxygen concentration cc/l	0.2
Water resistivity, ohm-cm	100,000 to 300,000

At the conclusion of the test, the apparatus was disassembled and the plates inspected and photographed (Figure 7). The uncharged plates had a tightly adherent thin film which is characteristic of good corrosion resistant samples in such an environment. The negatively charged zirconium plates had a tightly adherent film which appeared to be much less than that on the uncharged zirconium. The negatively charged stainless steel plates were perfectly clean with a black matte surface appearance. The positively charged zirconium plates and the positively charged stainless steel plates had very generous deposits of a dark brown solid. This solid, while not being as tightly adherent as a film, was well bonded to the plate and scraping with a sharp tool was necessary to dislodge the deposits.
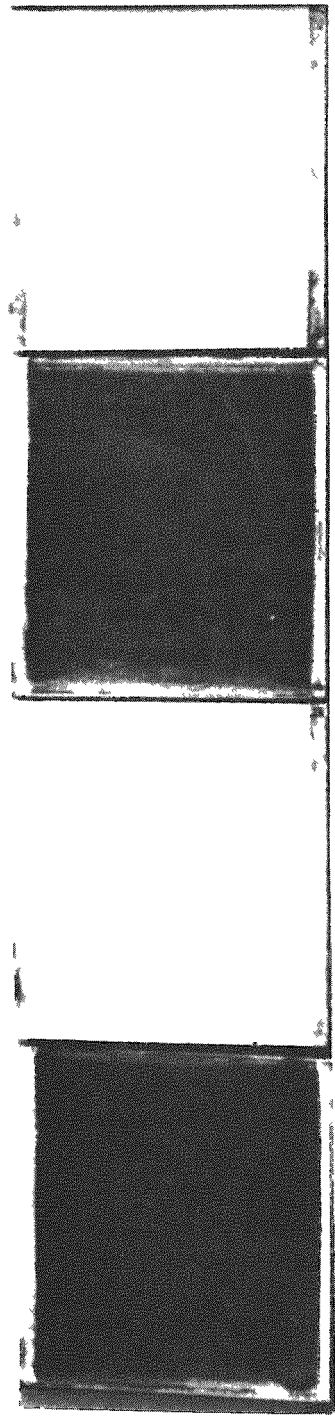
FIG. 6
APPEARANCE OF TYPE 347 STAINLESS STEEL PLATES
TESTED FOR 32 HR IN 240 F WATER AT 315 PSIG

| FLOW → | UNCHARGED Zr | CHARGED Zr | UNCHARGED SST 347 | CHARGED SST 347 |

ZIRCONIUM

UNCHARGED

+ CHARGE

− CHARGE

TYPE 347 STAINLESS STEEL

UNCHARGED

+ CHARGE

− CHARGE

FIG. 7
APPEARANCE OF CHARGED AND UNCHARGED ZIRCONIUM
AND STAINLESS STEEL SAMPLES TESTED FOR 362 HR
IN 450 F WATER AT 27 FPS AND 1000 PSI.
VOLTAGE ACROSS CHARGED PLATES = 1.0 V.

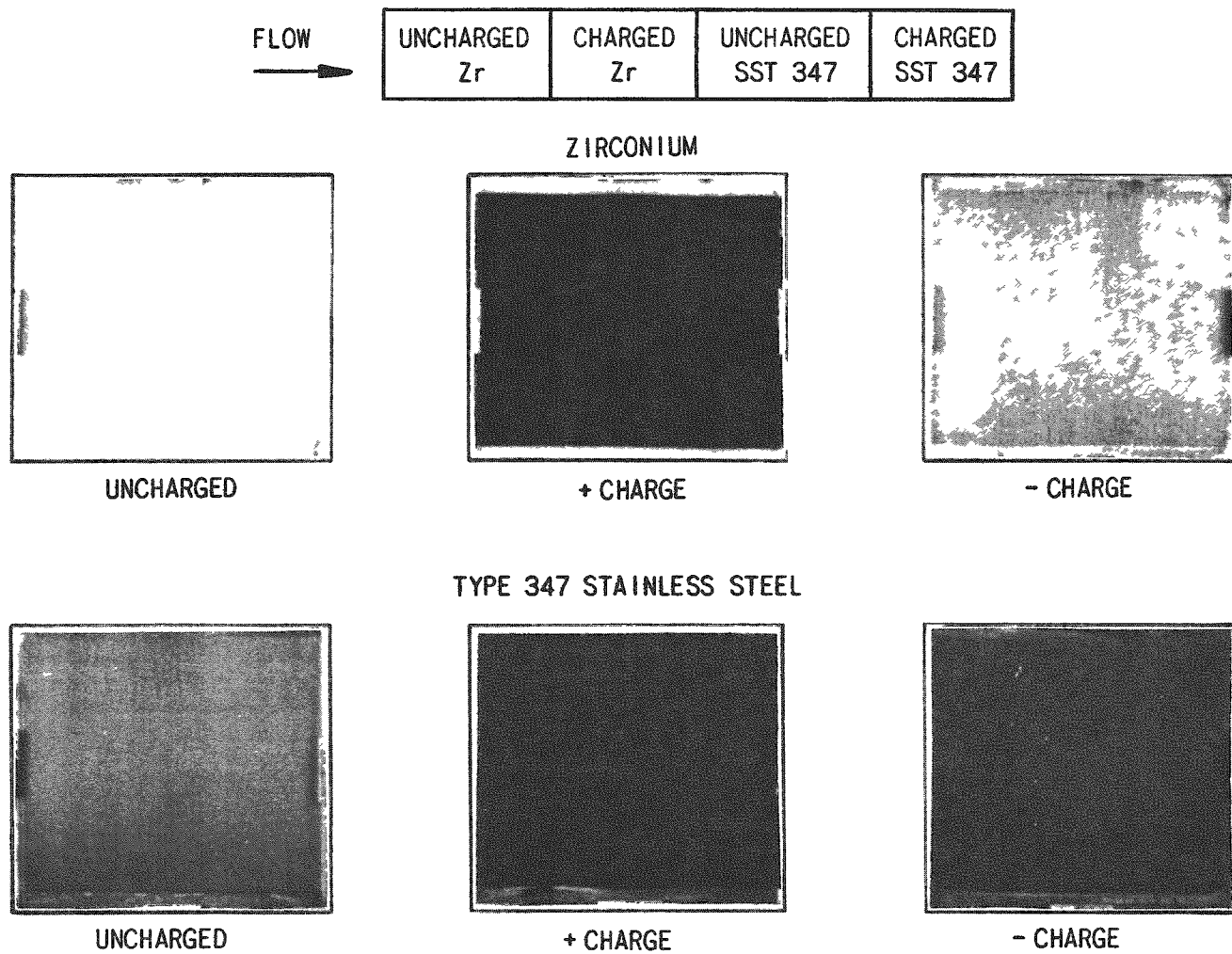The deposit on the stainless steel plates weighed 0.84 gm which represents a concentration of 42 mg/sq in. The deposit on the zirconium plates weighed 1.01 gm which represents a concentration of 50 mg/sq in.

X-ray diffraction showed that the deposits removed from the stainless steel and zirconium plates were identical and were essentially cupric oxide. Wet chemical analysis of deposit from a zirconium plate showed 58.2 per cent copper and 5.41 per cent iron. The deposit showed a weak attraction for a laboratory-type horseshoe magnet. The deposit from the stainless steel plate yielded the following spectrographic analysis:

Element	Per cent
Fe	10
Cu	>20
Pb	2
Ni	1
Cr	0.4
Mn	4
Zr	0.1
Al	0.4

Pressure drop data are plotted in Figure 8. It is noted that the pressure drop across the uncharged sections remained essentially constant throughout the test. The charged zirconium section suffered a very large increase in pressure drop in the first 60 hr of running time, leveled off, and then slowly rose. The charged stainless steel section showed the same general character except that the sharp rise in pressure drop took place after the zirconium pressure drop was essentially saturated.

The current drawn by the charged plate was recorded, but due to the poor water resistivity during the first 100 hr of the run, the current fluctuated considerably.

C.   Test No. 3 (SOS Test)

In view of the existence of a large quantity of copper observed in the Bilgewater Test, it was decided to repeat the test in a loop which was known to be quite clean. It is not to be inferred that the Bilgewater Test was performed in an "as is" loop, but it is fact that the loop had been cleaned by various and sundry cleaning agents. The Small Scale Heat Throughput Loop was cleaned by mechanical filtration followed by circulating a hot, strong solution of nitric acid. Repeated flushing with water was undertaken to remove the last trace of nitric acid. The operating variables for the SOS Test were as follows:
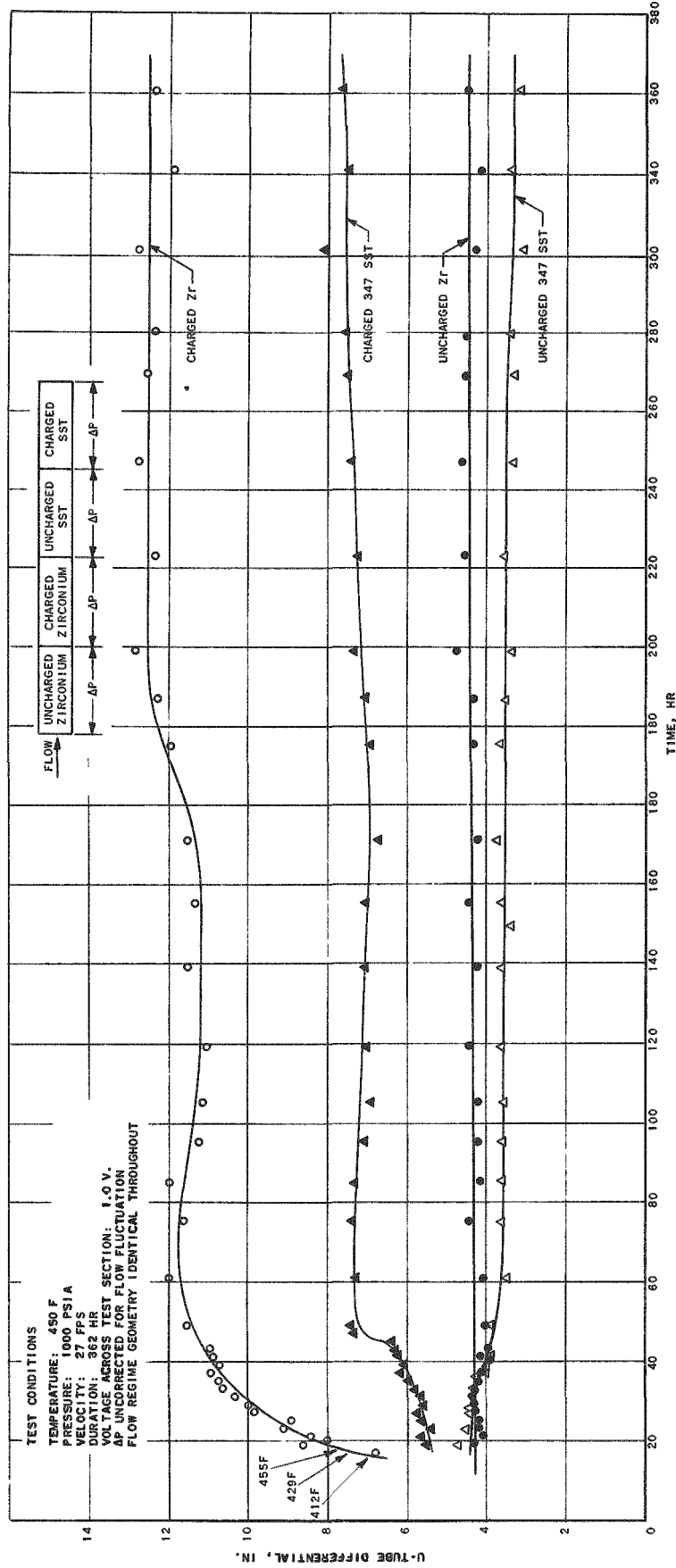
FIG. 8
PRESSURE DROP ACROSS CHARGED AND UNCHARGED
ZIRCONIUM AND STAINLESS STEEL PLATES. BILGEWATER TEST.

NR-G-3092-8

W.FAGAN:LRD,9-24-52

TEST CONDITIONS

TEMPERATURE: 450 F
PRESSURE: 1000 PSIA
VELOCITY: 27 FPS
DURATION: 362 HR
VOLTAGE ACROSS TEST SECTION: 1.0 V.
ΔP UNCORRECTED FOR FLOW FLUCTUATION
FLOW REGIME GEOMETRY IDENTICAL THROUGHOUT

U-TUBE DIFFERENTIAL, IN.

TIME, HR

16

Velocity	25 fps
pH	5-6
Resistivity	200,000 to 500,000 ohm-cm
Temperature	450F
Pressure	1000 psia
Oxygen concentration	0.2 cc/1
Voltage across test section	1.0 d-c

The test began October 21, 1952, and was concluded two weeks later. The uncharged and negatively charged zirconium plates have a characteristic tightly adherent, iridescent appearance. The positively charged zirconium plate has, superimposed upon its film, small specks of solid which look not unlike the appearance of a plate sprinkled with finely divided black pepper. The mass quantity appears very small but the "pepper" is definitely present and very loosely adherent. The rubbing of a finger across the surface is sufficient to remove the "pepper."

The positively and negatively charged stainless steel plates have generous quantities of deposits upon them. The appearance of the positively charged plates seems identical to the Bilgewater deposition color, whereas the negatively charged plates have the same type deposit but dark olive in color. The uncharged stainless steel plate has a fine filamentary deposit on it which is loosely adherent. The deposit is similar to the iron powder-horseshoe magnet experiment described previously. Traces of the deposit pattern look not unlike that of the macro grain structure of the plate. The positively charged stainless steel deposit weighs 46 mg which represents a deposition density of 2.3 mg/sq in., while the negatively charged stainless steel deposit weighs 96 mg which represents a deposition density of 4.8 mg/sq in. The weight gain on all other plates is negligible as compared to the charged stainless steel plates. The results of spectrographic analysis of the deposits on the positively charged stainless steel plates are tabulated.

Element	Per cent
Fe	25
Ni	3
Cr	2
Cu	6
Pb	10
Mn	15

The results of spectrographic analysis of the deposits on the remaining plates are tabulated in terms of approximate relative magnitude of concentration of elements on the respective plates.

Element	−347	uncharged 347	+Zr	−Zr	uncharged Zr
Fe	5	50	4	Typical	Typical
Ni	2	4	0.8	Zr film	Zr film
Cr	5	3	0.5		
Cu	50	2	5		
Pb	1	0.5	6		
Mn	3	0.4	5		
Zr	0.3	<0.1	0.4		

The pressure drop data are shown in Figure 9. The same general characteristics as in the Bilgewater Test pressure drop are noted; however, the percentage increase in pressure drop is not as great as in the case of the heavier deposition noted in the Bilgewater Test.

D. Test No. 4 (Operation Slushpump)

1. Introduction

Based on past experiments using charged plates, Test No. 4 known as "Operation Slushpump" was made to determine whether fortuitously located charged plates could act through a distance and prevent deposition of solids on a long fuel element.

2. Test Apparatus and Procedure

The test assembly consists of a series of long and short typical fuel element sections (Figure 10).

A typical long section consists of 14 zirconium plates, 0.087 in. by 2-3/8 in. by 43.5 in. The plates are mounted parallel to each other on zirconium spacers to provide the flow channels. The zirconium plates and covers are placed in a Type 304 stainless steel box which is designed to hold the plates without movement and yet permit disassembly at will. The area available for water flow is represented by 13 rectangles, each measuring 0.087 in. by 2.25 in. To insure positive electrical contact, small tackwelds are made by binding zirconium to zirconium and zirconium to stainless steel. Two long assemblies are made: one is used as a control section to determine deposition that would take place without the influence of the electrical field; and the second is called the charged section. It is desired to protect the charged section by means of two short sections which are placed at the upstream and downstream ends of, and electrically insulated from, the long charged section. As shown in Figure 11, water flows into the long control section, enters the upstream charged section, continues through the long charged section and out again through the downstream charged section. By charging the small sections positively with respect to the long charged section, deposition on the latter may be minimized or prevented.

W.FAGAN:F.J.S.,12-5-52
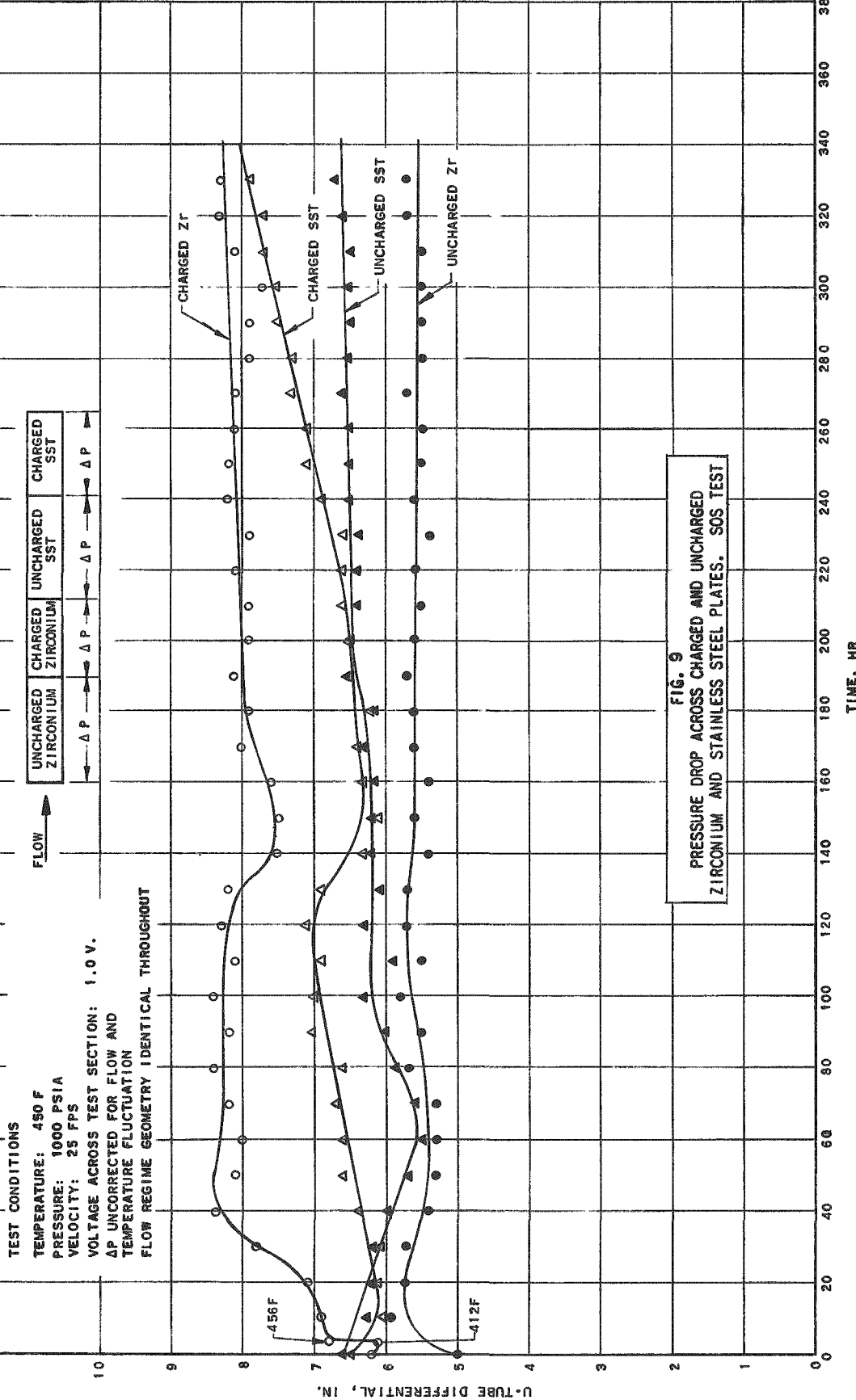
FIG. 9

PRESSURE DROP ACROSS CHARGED AND UNCHARGED
ZIRCONIUM AND STAINLESS STEEL PLATES, SOS TEST

NR-7-10102-B

TEST CONDITIONS

TEMPERATURE: 450 F
PRESSURE: 1000 PSIA
VELOCITY: 25 FPS
VOLTAGE ACROSS TEST SECTION: 1.0 V.
ΔP UNCORRECTED FOR FLOW AND
TEMPERATURE FLUCTUATION
FLOW REGIME GEOMETRY IDENTICAL THROUGHOUT
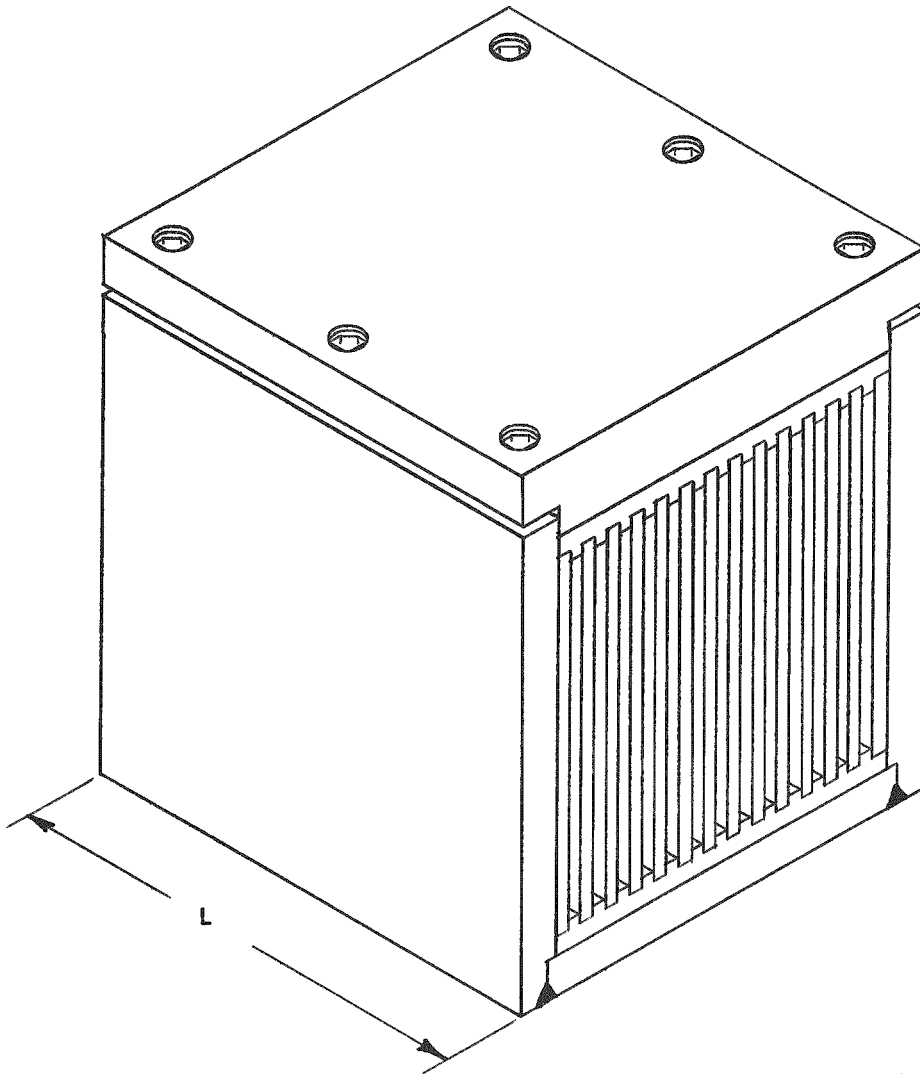
LONG ASSEMBLY L = 43.5"
SHORT ASSEMBLY L = 3"

FIG. 10
14-PLATE TEST SECTION

RE-7-10803-A
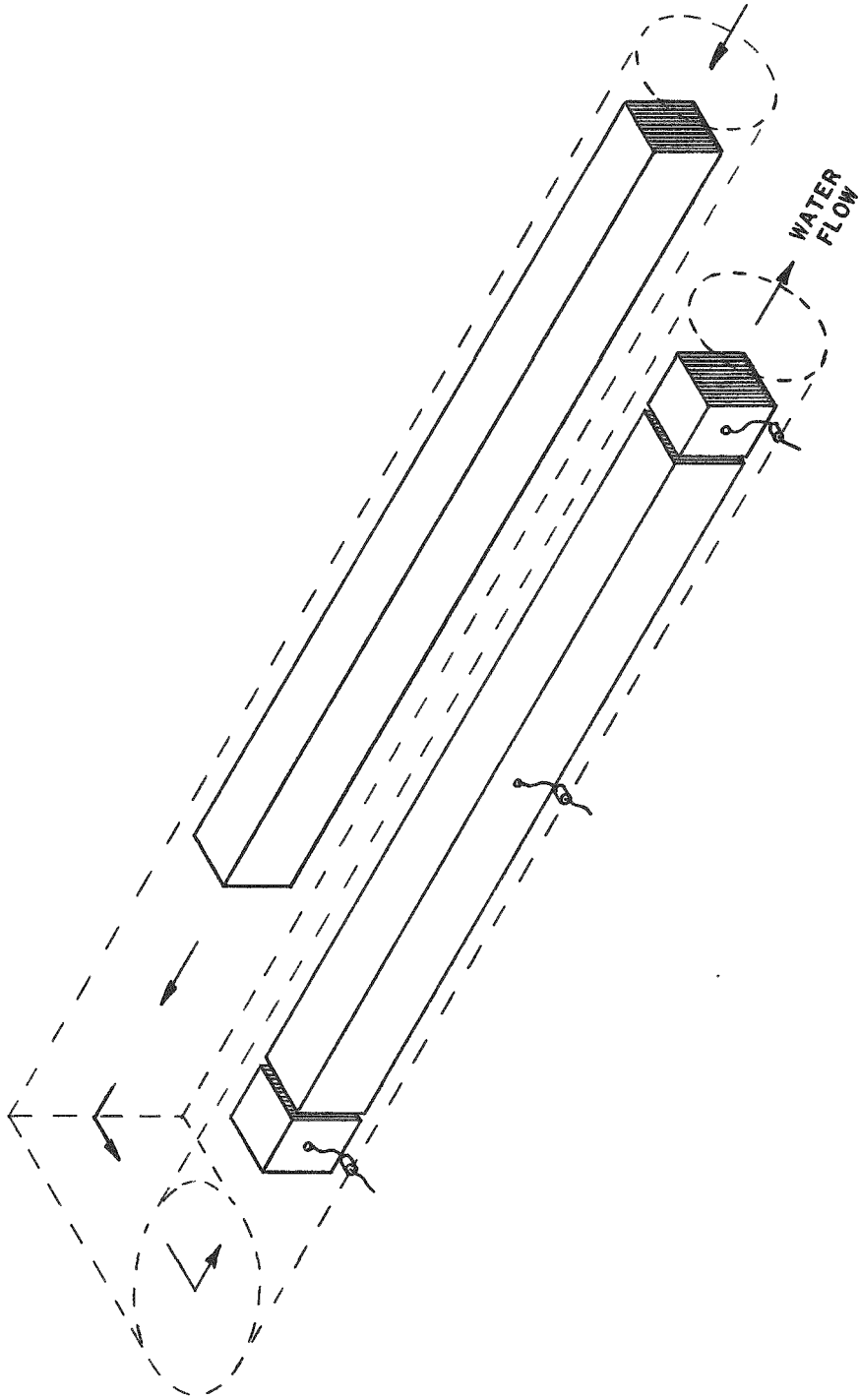
FIG. II
SCHEMATIC DIAGRAM OF
SLUSH PUMP TEST ASSEMBLY

WATER
FLOW

W.S.FAGAN:G.C.D.,4-22-53

The long control test section is mounted in a 6-inch Schedule 40 stainless steel pipe. Welding rings located near the extremes of the pipe are used to position the test section. A limiting stop is bolted in place to prevent movement of the section and a Teflon gasket seals off leakage water flow, insuring that all flow through the pipe will be diverted through the plate section. Openings are provided in one welding ring so that compression exists on the plate assembly at all times.

The long, charged test section, along with the two short charged sections, is similarly inserted in a 6-inch pipe with gaskets, seal, and limiting stop. The long section is at ground potential. The gap between the sections is 3/32 in. with each 14-plate section coplanar with the adjoining section.

The assembly of the short sections is identical to the long sections, the only essential difference being that water flows past a 3-inch length as opposed to a 43.5-inch length in the long assembly.

Electrical connections are made from the three charged sections by means of stainless steel wire through Teflon-insulated fittings in the pipe wall. Pressure taps are installed so that pressure drops across the two pipe sections can be measured.

The test assembly is bolted to a superstructure and base plate designed to accommodate a bottom ring located in the pressure vessel of the Large Scale Component Test Facility. The test assembly is shown in Figure 12. Pressure tubing is brought through the pressure vessel wall. All pressure drop measurements were made with a Barton differential pressure gage and valve manifold.

Gold wire insulated in Teflon tubing was used to connect the three voltage leads from the charged test section terminals to the instrument thimble in the pressure vessel. The potential source was a No. 6 dry cell battery with potential rheostat control.

All zirconium plates were pickled before test in nitric acid-hydrofluoric acid. Prior to test, the loop was cleaned with citric acid, versene, oxalic acid, and water.

On February 24, 1953, Operation Slushpump began and formally ended 14 days later. The test conditions were:

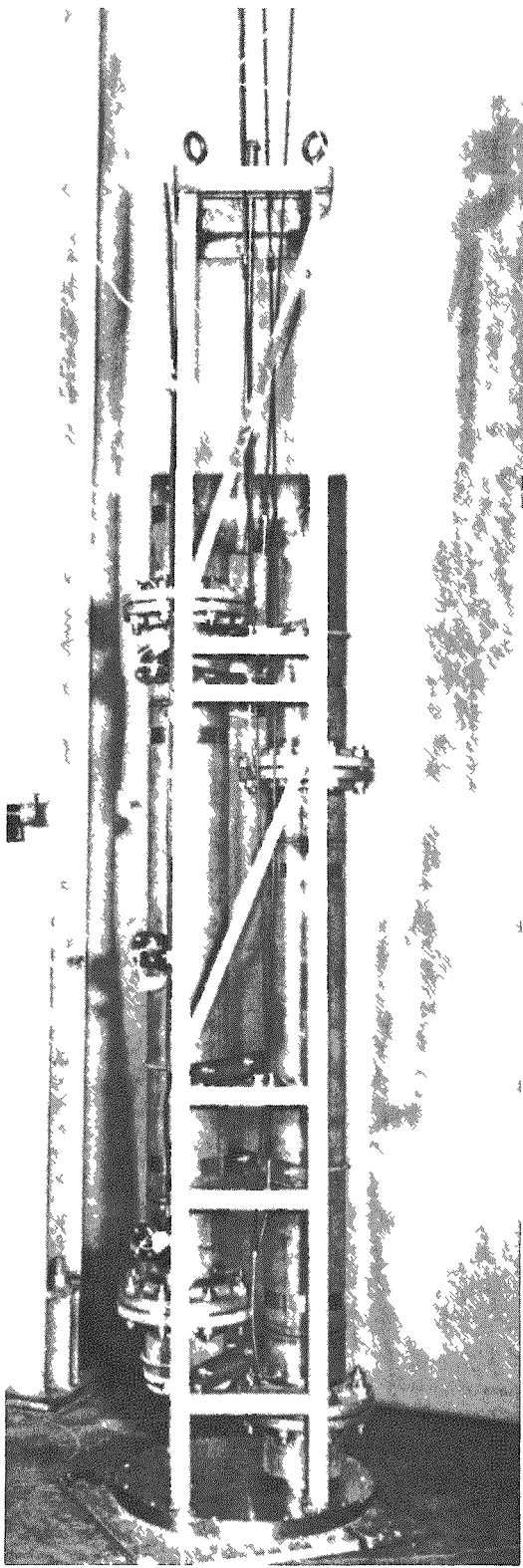|	
System Pressure	1000 psig
System Temperature	450F
Flow Rate	190 gpm corresponding to a linear velocity of 24 fps.
Dissolved Oxygen Concentration	0.2-0.7 cc/1
pH	6-7

FIG. 12
SLUSHPUMP TEST ASSEMBLY

Water Resistivity	110,000 ohm-cm at startup
	290,000 ohm-cm at 24 hr
	500,000 ohm-cm at 48 hr
	1,000,000 ohm-cm
Charged Section Voltage	1.3

Milliameter readings followed the changes in resistivity quite well. The pressure drop readings are not significant even though they were essentially constant.

At 118 hr after start-up, the upstream charged section first electrically opened and then shorted out. Since operational procedure for shutdown is complex, the decision was made to keep the test running rather than to shut down and inquire into the nature of the malfunction. It was hoped that the remaining charged section would show a significant protective effect.

3. Results

At the end of the run the loop was depressurized, drained, and the test section removed from the pressure vessel.

It was found that the upper section had shorted out because of a failure of the gold wire at the point where the wire was screwed into the thimble of the pressure vessel. The wire first broke, causing an open circuit and immediately thereafter the free end grounded out. Upon inspection of the individual plates in the assembly, it was found that all 56 zirconium-to-zirconium tack welds had corroded very seriously due to contamination of the inert atmosphere used in the dry box welding. Furthermore, the weld corrosion and the complete lack of penetration of the welds caused 7 of the 14 plates in the downstream charged section to fall out of its cartridge and they were picked up from the bottom of the pressure vessel. Inspection of the plates in the long assemblies showed that severe buckling and warping of the plates had occurred. While positive alignment was provided at four positions along the length, three sections were unsupported and distorted, therefore, the pressure drop data gave no clue to deposition. Explanation of this buckling cannot be made in terms of thermal expansion or stress relief. Visual examination of the long, charged and uncharged plates showed no appreciable difference.

The shorted-out upstream charged section had a small loose deposit of a black solid on the edge adjacent to the long assembly. Evidently, deposition had taken place in the first 118 hr and was either partially swept away afterwards or else the deposition observed was accumulated in 118 hr. The small downstream charged plates which had fallen out had no deposition and looked quite clean with the usual temper film. The seven plates which remained intact had a heavy coating of black solids at the leading edge of the plate adjacent to the charged long section and the solid extended 1/16 to 1/8 in.

downstream of this edge (Figure 13). It is significant that the two plates adjacent to the cavity produced by the loss of the plates had the heaviest deposition which extended the furthest back. This might be due either to the lower velocity or to the favorable alteration of the electric field by the loss of the plates.

Analyses of the deposition and the loop water are tabulated:

Elements	Deposition, Per Cent	Loop Water, Parts Per Billion
Aluminum	0.2	15
Barium	---	5
Calcium	<0.02	150
Chromium	0.1	2
Cobalt	<0.1	<5
Copper	65	150
Iron	2	150
Lead	2	40
Magnesium	<0.02	50
Manganese	1	5
Nickel	1	10
Silicon	1	1500
Silver	<0.1	<5
Sodium	---	300
Strontium	---	0.5
Tin	<0.2	<20
Zinc	<0.5	40
Zirconium	4	<10

IV. DISCUSSION

A. Test No. 1 (Preliminary Test)

The test showed that a preferential deposit is possible and, under the conditions of the test, it is noted that lead was removed in greater quantities than iron from the loop by a factor of 2-1/2 to 1.

B. Test No. 2 (Bilgewater Test)

The Bilgewater test showed the unexpected existence of large quantities of copper in the test loop. The fact that the large quantities were deposited shows that the procedure would be excellent under these operating conditions, for the removal of the transported material. The redox mechanism is ruled out in the deposition because a deposit of copper would not plate out on a positively charged plate. The colloidal deposition mechanism

FIG. 13
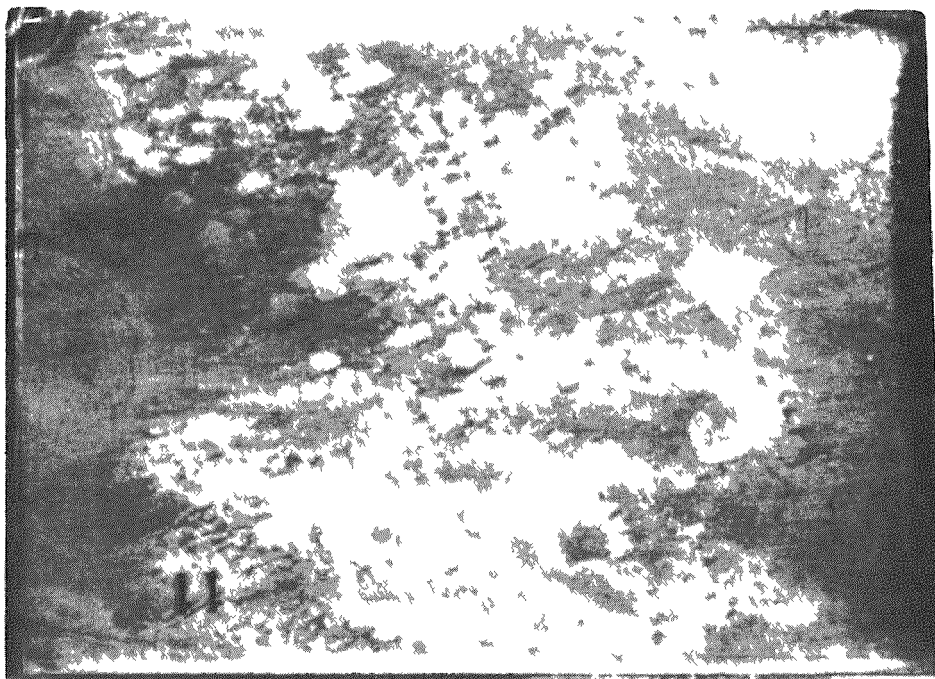DEPOSITION ON DOWNSTREAM CHARGED PLATE

as postulated earlier seems consistent with the two factors that the deposition on both stainless and zirconium plates is identical, and also that the zirconium plates had more deposition than its downstream neighbor, the stainless steel plates. It might be inferred that the downstream plate "saw" cleaner water.

The appearance of the two negatively charged plates looks most attractive. This would rule out the deposition of positive metallic ions since no deposition could be seen. It immediately suggests that the negative plate is a protected plate and it might be possible to negatively charge a critical location in the flow stream in order to prevent deposition of solids. It was noted that the leading edges of all uncharged plates have heavier films than the trailing edges.

The Bilgewater pressure drop data are plotted in Figure 8. The fact that the uncharged stainless and zirconium sections have a constant pressure drop throughout the run is evidence for the lack of deposition on the plates. The pressure drop curve for charged zirconium shows a marked rise at the beginning of the run with perhaps a 1-1/2-fold increase in the first 60 hr. Because of the fact that zero time represents a cold loop, and since the operating temperature was reached at 20 hr with a large time rate of pressure drop increase at that time, it seems likely that this large pressure drop change occurred in perhaps 45 hr. One must not necessarily assume that the leveling off of the curve means that no deposition is taking place but rather that the worst case of surface roughness has been achieved and deposition can take place at constant surface roughness with relatively little decrease in water flow area. The charged stainless pressure drop has the same general character although the large time rate of increase takes place at about 45 hr which seems to indicate that, as the upstream zirconium plates saturate, the downstream plates "carry the ball." The fact that the stainless pressure drop is smaller than the zirconium pressure drop and that the zirconium has leveled off and the stainless is very slowly rising, leads to the conclusion that eventually the two curves would coincide.

C. Test No. 3 (SOS Test)

The SOS Test results showed some similar features to Bilgewater and also marked differences. These differences are largely due to the pH differences in the two tests. The pH in the SOS Test was on the acid side while Bilgewater was neutral. The acid cleaning given to the Small Scale Heat Throughput Loop left adsorbed and absorbed acid in packings, gaskets, etc., which was slowly liberated and tended to lower pH in the test. The ion bed did not seem effective in removing the hydrogen ion, as is shown by data of pH before and after the exchange column.

It is a known experimental fact that hydrogen ion concentration can affect the quantity and even the sign of the charge carried by a colloidal particle. It seems reasonable that the high hydrogen ion concentration in

the SOS Test caused by adsorption of hydrogen ions on copper colloids resulted in a relatively large deposition of copper on the negative Type 347 plate. Evidently manganese, iron, and lead are not as markedly disturbed by this since the positive Type 347 plate is quite rich in these constituents.

The fact that zirconium did not behave in the same manner as the stainless steel is disturbing. It is true that the positive zirconium plate was rich in copper, lead, and manganese, but the quantity of deposit was small and had a discontinuous nature as mentioned. It is possible that the bonding between deposited solid and temper film fails at a low pH.

The decrease in pressure drop across the charged plates at 140 hr is probably due to an unknown flow disturbance, such as a water hammer, which would tend to dislodge the deposit. The recovery from this shock is speedy.

D. Mathematical Analysis

The following represents a calculation of the history of a charged particle in an electric field subject to a turbulent-type resisting drag.

Consider a particle of mass, M, moving from left to right between two charged plates in a fluid traveling with uniform velocity, u_0, in the + x direction as shown in the illustration. The plates are located at y = 0 and
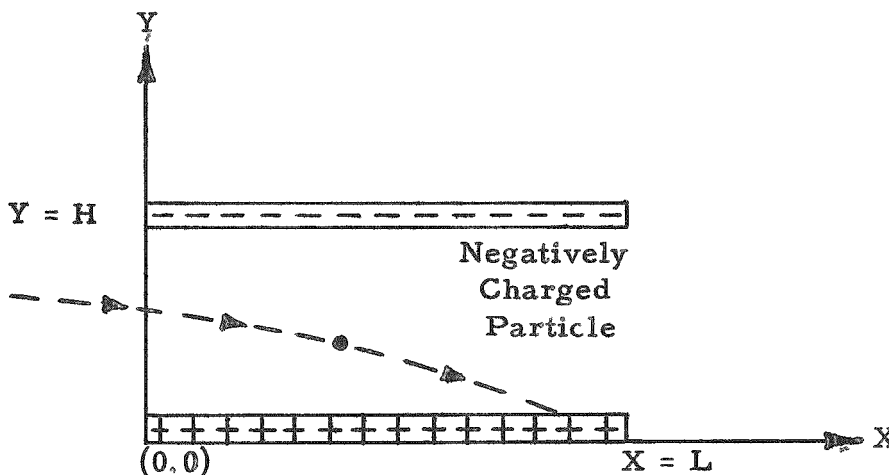
y = H and extend from x = 0 to x = L. Under the influence of electric, drag, and inertial forces, the trajectory is indicated by the dotted line. The electric force is given as the product of field intensity and charge carried by the particle in question and is directed in the -y direction.

$$\text{Electric force} = ne\left(\frac{V}{H}\right) \tag{1}$$

where   n = number of electronic charges carried by the particle
        e = absolute value of the electronic charge,
        V = voltage difference between the plates

The effect of space charge on the field is neglected since it is small and would require a solution of the Poisson Equation which would not be justified in view of the poor value of n which is to be used and because of the lack of accuracy needed in the final result.

The drag force is taken as acting in the + y direction and varying with the square of the y component of velocity. This is somewhat arbitrary but it must be realized that the colloidal particle is moving with the stream without slip and deviations from its y velocity component cause the drag. Further, the flow is in a turbulent regime and it would be presumptuous to use the classical Stokes Law for viscous regime drag.

$$\text{Drag Force} = (4\pi r^2)\ C\left(\frac{dy}{dt}\right)^2 \tag{2}$$

where
- r = radius of the spherical particle
- t = time coordinate
- C = drag coefficient

The inertial force is given in terms of the mass of the particle, M,

$$\text{Inertial Force} = M\frac{d^2 y}{dt^2} \tag{3}$$

To solve for the trajectory, the dynamic equations are written for the x and y directions

$$M\frac{d^2 x}{dt^2} = 0 \tag{4}$$

$$-ne\frac{V}{H} + 4\pi r^2\ C\left(\frac{dy}{dt}\right)^2 = M\frac{d^2 y}{dt^2} \tag{5}$$

Equation (4) is integrated with velocity u_o and position $x = 0$ at $t = 0$.

$$\frac{dx}{dt} = u_o \tag{6}$$

$$x = u_o t \tag{7}$$

Equation (5) is integrated using $dy/dt = 0$ and $y = y_o$ at $t = 0$.

$$\frac{dy}{dt} = -\left[\frac{neV}{4\pi r^2\ HC}\right]^{1/2}\ \tanh\ \left[\frac{4\pi r^2\ CneV}{M^2 H}\right]^{1/2} t \tag{8}$$

$$y_o - y = \frac{M}{4\pi r^2\ C}\ \ln \cosh\ \left[\frac{4\pi r^2\ CneV}{M^2 H}\right]^{1/2} t \tag{9}$$

The equations can be combined and simplified by using (7), (10), and (11).

$$M = (4/3)\pi r^3 p \tag{10}$$

$$n = 4\pi r^2 a \tag{11}$$

where "p" is the mass density of the particle and "a" is the number of electronic charges per unit area borne by the particle.

$$y_0 - y = \frac{pr}{3C} \ln \cosh \frac{3x}{pr\, u_0} \left[\frac{CaeV}{H}\right]^{1/2} \tag{12}$$

Set Y equal to the largest y_0 trapped.

$$Y = \frac{pr}{3C} \ln \cosh \frac{3L}{pr\, u_0} \left[\frac{CaeV}{H}\right]^{1/2} \tag{13}$$

The efficiency, F, can be introduced

$$F = \frac{Y}{H} = \frac{pr}{3HC} \ln \cosh \frac{3L}{pr\, u_0} \left[\frac{CaeV}{H}\right]^{1/2} \tag{14}$$

A useful approximation can now be used

$$\ln \cosh x = x \tag{15}$$

Equation (15) is valid for large arguments, as is shown in Figure 14.

Using Eq. (15), Eq. (14) becomes

$$F = \left(\frac{L}{H}\right)\left(\frac{1}{u_0}\right)\left[\left(\frac{V}{H}\right)\frac{ae}{C}\right]^{1/2} \tag{16}$$

It is noticed that the efficiency for large arguments in Eq. (14) is independent of particle size. The physical significance of this is apparent from the differential equation (5). The electric force varies as r^2, the drag force varies as r^2, but the inertial force varies as r^3. Thus, if the inertial force is neglected, a radius independent differential equation results which, when integrated, yields the result identical to the asymptotic result, Eq. (16) given for large arguments.
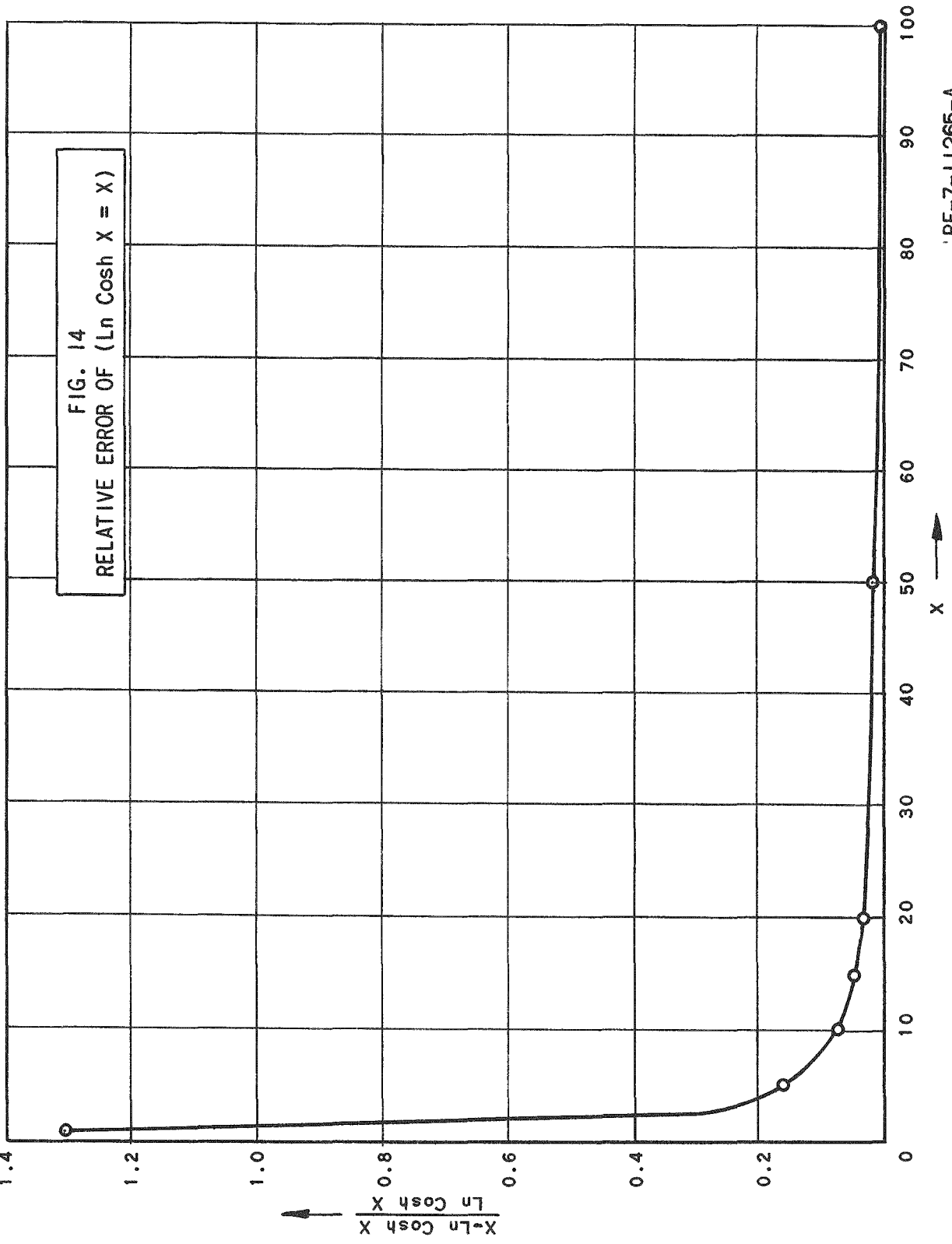
Examination of Eq. (5) can give a qualitative picture of the behavior of efficiency versus particle size, all other things being equal. The curve is independent of radius for values of r from zero upwards until the radius gets so large that the inertial force can no longer be neglected. At this radius, the efficiency starts to drop with increasing radius and does so monotonically. Numerical values may be inserted in Eq. (16).
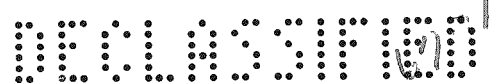
L = 6.35 cm u_0 = 762 cm/sec (25 fps)
H = 0.221 cm   V = 1 practical volt

FIG. 14
RELATIVE ERROR OF (Ln Cosh X = X)

W.FAGAN:G.D.,6-25-53

RE-7-11265-A

$\dfrac{X-Ln\ Cosh\ X}{Ln\ Cosh\ X}$

X

The value of C is taken from experimentally determined drag coefficients.
At unit Reynolds Number and as defined, $C = 2.64$ gm/cm^3. This is conservative, with a smaller value not unlikely. Due to the approximations used, and since C appears to the $-1/2$ power, it is a reasonable value.

The value of "a" is the weakest link in the chain. Since it is an experimental quantity and a function of many variables, and since no experiments have been performed, a guided guess must be made. Experiments[2] have been performed on Fe_2O_3 colloids at room temperature in water, to determine the migration velocities in a voltage gradient. Data were presented in terms of mobilities, the ratio of velocity to field strength. To adapt for our application, the electric and viscous regime drag forces are equated.

$$(6\pi\mu ur) = neE \tag{17}$$

where 　　　μ = the viscosity of the fluid
　　　　　　E = the field strength.

$$ae = \frac{3}{2}\frac{\mu}{r}\left(\frac{\mu}{E}\right) \tag{18}$$

Set $\mu = 0.01$ gm/cm sec for water

$$\frac{u}{E} = 3.5 \; 10^{-4} \; \frac{cm^2}{volt \; sec}$$

from the data

$$r = 10^{-6} \; cm$$

No particle size data appear in the paper and it is estimated that 0.01 microns is reasonable.

From Eq. (18),

$$ae = 5.25 \; \frac{gm}{volt \; sec^2}$$

The efficiency of the deposition is calculated from Eq. (16).

$$F = 0.053 \tag{19}$$

To check the validity of Eq. (15), the argument of Eq. (14) is evaluated at $r = 10^{-4}$ cm.

$$p = 5.18 \; \frac{gm}{cm^3} \quad \text{for } Fe_3O_4$$

Argument = 383 so Eq. (15) is most valid.

---

[2]F. Hazel and G. Ayres, "Migration Studies with Fe_2O_3 Sols," J. Phys. Chem. 35, 2930 (1931).

Bilgewater yields data from which efficiency may be calculated. Assume that the efficiency is independent of concentration and particle size. Let W be the mass of changed particles entering the test section, W_1 the deposition on the upstream charged plates, and W_2 the deposition on the downstream plates.

$$WF = W_1 \qquad (20)$$

$$F\,W(1-F) = W_2 \qquad (21)$$

Combining Eqs. (20) and (21), the final result is obtained.

$$F = 1 - \frac{W_2}{W_1} \qquad (22)$$

From the data, $W_1 = 1.01$ gm and $W_2 = .84$ gm

$$F = .17 \qquad (23)$$

This result may be compared with Eq. (19).

The calculation showing a 5 per cent efficiency indicates that the cleaning up process could be improved considerably by decreasing the fluid velocity well below the 25 fps used in the calculation. A velocity of 1 fps would trap all particles since the efficiency would then go to 125 per cent. Conceivably a filter with such high efficiency could be installed in a low flow bypass circuit.

V. RECOMMENDATIONS

The mechanism of the transport corrosion product deposition is of great interest. Since back voltages have been observed, as reported earlier, and since the SOS Test showed that the nature of the deposit, both as to quantity and appearance, differs considerably on the zirconium and the stainless steel plates, the nature of the surface is important and extraneous electrochemical effects at the phase interface must be minimized. Thus for future experiments the use of metallic gold, charged surfaces is recommended. Experiments could be performed using charged plate sections in series with the linear velocity being the only varied parameter. Equation (16) shows that the efficiency of the postulated mechanism varies inversely as the inlet velocity and this one experiment in itself should be enough to show whether this mechanism is a reasonable one. The other parameters which appear in Equation (16) could also be checked.

Another suggestion is that the particle size of the deposition product may be increased by the deposition in a Bilgewater-type experiment. Furthermore, it may be possible to dislodge the collected particles from the charged plates by a reversal of polarity. Assuming that the above stated facts are valid, which can be shown by experiment, one could conceive of a trapping mechanism for finely divided solids by means of the following procedure:

1.   Operate a charged plate section with a given polarity for 60 hr at which time a heavy deposit will have taken place on the positively charged plate.

2.   Reverse polarity and cause the fluid flow through the section to be diverted through a mechanical filter which would effectively remove the large diameter particles.

3.   Remove and clean the line filter from the standby unit which would operate in parallel with the previously mentioned filter.